Asian Journal of Chemistry; Vol. 37, No. 4 (2025), 795-803

ASIAN JOURNAL OF CHEMISTRY

https://doi.org/10.14233/ajchem.2025.33330

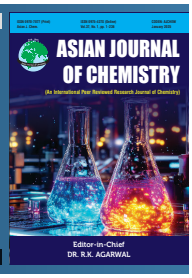

Molecular Structural, Spectral and HOMO-LUMO Analysis of Acemetacin in Aqueous Phases: A Density Functional Theory Study

B. YOGESWARI[1,*], S. DEIVANAYAKI[2], A. SAJITHA BANU[3], V. UMADEVI[4], V. REGINA DELCY[4] and A. VENKATRAJ[5]

[1]Department of Physics, Sri Eshwar College of Engineering (Autonomous), Coimbatore-641202, India
[2]Department of Physics, Sri Ramakrishna Engineering College (Autonomous), Coimbatore-641022, India
[3]Department of Physics, PSNA College of Engineering and Technology (Autonomous), Dindigul-624622, India
[4]Department of Physics, Dr. Mahalingam College of Engineering and Technology, Pollachi-642003, India
[5]Department of Physics, Sri Krishna College of Technology(Autonomous), Coimbatore-641042, India

*Corresponding author: E-mail: yogeshwari.b@sece.ac.in

Received: 7 January 2025; *Accepted*: 20 February 2025; *Published online*: 29 March 2025; AJC-21939

Polar and non-polar solvents like water (ε = 78.5), ethanol (ε = 24.852), acetone (ε = 20.493) and diethyl ether (ε = 4.24) were employed to study the solubility of acemetacin, which is a non-steroidal anti-inflammatory drug (NSAID) through quantum density functional theoretical studies using B3LYP/6-31G(d) level. In present study, acemetacin was optimized in the gaseous phase and further explored in the solution phase environments. The characteristic parameters of acemetacin such as bond lengths, bond angles, total energy, dipole moment, thermal energies, specific heat, entropy and zero point vibrational energy in gaseous and solution phases were computed. The energy difference between most stable [acemetacin in water (AMN-W)] and the least stable structure [acemetacin in diethyl ether (AMN-D)] was found to be 3.76 Kcal/mol. The zero point vibrational energy of acemetacin in gas phase is found to be 225.05 Kcal/mol. The fundamental vibrational frequency analysis of acemetacin has been done by using B3LYP/6-31G(d) level and compared with the harmonic vibrational frequencies. The HOMO-LUMO analysis of acemetacin has also been investigated. The molecular electrostatic potential (MEP) map was applied to study the distribution of charge density and the location of the chemical reactivity of acemetacin.

Keywords: Acemetacin, Self-consistent reaction field theory, Vibrational modes, Diethyl ether.

INTRODUCTION

Among the variety of available NSAIDs, indometacin and its glycolic acid ester, acemetacin are regarded as effective drugs for treating post-operative pain, lower back pain and rheumatoid and osteoarthritis [1]. Acemetacin is known to be an aromatic heteropolycyclic compound known as benzoylindoles with 3 rings, 5 hydrogen acceptor and only one hydrogen donor units. Acemetacin is an ester of glycolic acid of indometacin and 50-90% of engrossed acemetacin in a human body is rehabilitated into indomethacin; its bioconvertible metabolite [2]. Acemetacin is also used for the treatment of ankylosing spondylitis, joint exasperation and irritation in spinal column, aching inflammation, swelling due to injury and other musculoskeletal disorders [3].

Acemetacin is a long-duration NSAID [4,5] and it has a strong affinity for plasma proteins and the portion of acemetacin available in the body with activeness (bioavailability) following the repeated oral doses almost twice daily is estimated roughly as 66% in plasma and 64% in urine.

The existence of a molecule in more than one crystalline structure in the solid state is known as polymorphism. Acemetacin is an active pharmaceutical ingredient (API) polymorph having carboxylic acid catemer and dimer O–H···O synthons. Sanphui *et al.* [6] compared the solubility of poorly soluble acemetacin polymorphs, including its inherent suspension in phosphate buffer and found that both polymorphs dissolving at the same rate. They found that acemetacin polymorphs dissolve at 37 ºC were 3.5 times faster than the monohydrate counterpart. Thus, the change to the hydrate reduced solute solubility after 1.5 to 2 h before the maximum solubility. The same research group [7] used mechanochemical methods to find solid acemetacin co-crystals and salts which are stable in water. Acemetacin hydrates across all solute-solvent interactions,

therefore they experienced the same problem as before. Single-crystal XRD was utilized to examine the *p*-aminobenzoic acid-acemetacin and acemetacine-isonicotinamide co-crystal structures. They resolved picolinamide, caprolactam and piperazine salt structures with acemetacin using high-resolution powder XRD data and concluded that the acemetacin-piperazine compound had the highest dissolving rate and best stability in the solution phase and excellent stability for an increased oral formulation of the drug. The outcomes of solute molecular energies in various atmospheres may elucidate the influence of solvents on molecular geometry and stability.

In light of these above facts, the present study intends to perform the quantum chemical calculations to determine the solubility of acemetacin in polar and non-polar solvents such as water, ethanol, acetone and diethyl ether, respectively. The optimized gas phase structure of acemetacin has been further utilized for the solvation study. The quantum chemical parameters of acemetacin such as bond lengths, bond angles, total energy, dipole moment, thermal energies, specific heat, entropy and zero point vibrational energy in gaseous and aqueous phases were calculated. The HOMO, LUMO and the molecular electrostatic potential (MEP) map of the titled molecule have also been investigated in gaseous as well as aqueous phases.

COMPUTATIONAL METHODS

Initially, the structure of acemetacin was retrived from the NCBI PubChem database [8]. In density functional theory (DFT) methods, the Becke's three parameter exact exchange functional (B3) [9] combined with gradient corrected correlation functional of Lee-Yang-Parr (LYP) [10] was employed to optimize the acemetacin molecule in gaseous and aqueous phases by implementing the 6-31G(d) basis set through Gaussian 09 software program [11]. The same method was used to investigate the thermal energies, specific heat, entropy and zero point vibrational energy of acemetacin in gaseous and aqueous phases. The vibrational wavenumbers, MEP map and the HOMO-LUMO energy levels of acemetacin were also computed with the above method. The vibrational wave number assignments of acemetacin were done with the help of Gaussview program [12]. The solute-solvent interface studies were carried out through the self-consistent reaction field theory (SCRF), supported by Tomasi's polarized continuum model (PCM) [13] at B3LYP/6-31G(d) level of theory. In this process, the titled molecule is positioned in the cavity within water (ε = 78.5), ethanol (ε = 24.852), acetone (ε = 20.493) and diethyl ether (ε = 4.24) as solvents.

RESULTS AND DISCUSSION

The optimized structure of acemetacin is given in Fig. 1 with atom labeling. For convenience, the acemetacin in gaseous and aqueous phases: water, ethanol, acetone and diethyl ether are named as AMN, AMN-W, AMN-E, AMN-A and AMN-D, respectively. Tables 1 and 2, respectively present the bond lengths and bond angles of acemetacin in gaseous and aqueous phases calculated at B3LYP/6-31G(d) level of theory. The indole ring in acemetacin is found to be planar; at the same time its

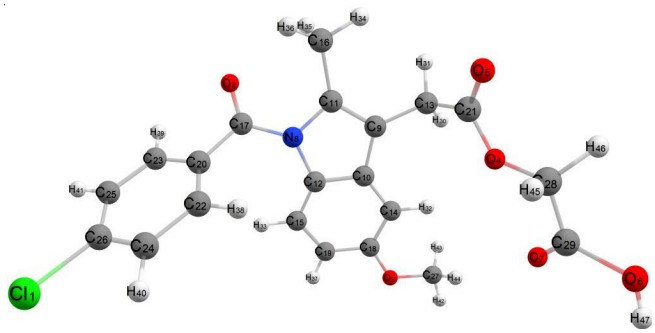

Fig. 1. Optimized structure of acemetacin with B3LYP/6-31G(d) level of theory

glycolic acid ester side chain and *p*-chlorine-benzoyl group possesses rotatable carbon-carbon bonds [14].

The aqueous phases do not affect the C-C bonds of AMN except a few. The solute-solvent interactions are often less than the intramolecular forces, which could be responsible for the minimal geometric changes as the solute moves from the gaseous to the liquid phases. Moreover, the chlorobenzoylic C-C bond is slightly compressed by 0.003 Å almost in all the aqueous phases. Only small stretching (0.001 Å) is observed in indolic and chlorobenzoylic C-C bonds as a result of solvation. The chlorobenzoylic chlorine-carbon (Cl1–C26) bond is slightly stretched by 0.004 Å. Distinguished variations are observed in the O-C bond lengths related to the methoxy oxygen of AMN. The O-C bonds associated with methoxy oxygen (O2) and acyloxy acidic acid carbons (C21 and C29) are compressed by 0.007 Å and 0.008 Å, respectively. The N-C bond lengths of AMN are affected only to a certain extent as result of solvation irrespective of the aqueous environments. The C-H bond lengths varied from 1.083-1.099 Å corresponding to indolic and methoxy C-H bonds, respectively.

The bond angles of the acetyloxy acidic acid C-O-C in acemetacin (Table-2) increase by nearly half a degree when immersed in water. Same trend is followed in the other aqueous phases such as acetone, ethanol and dietlyl ether as well. The chlorobenzoylic C-C-C bonds are also affected considerably in all aqueous phases compared to acemetacin in gas phase. The C-C-H bond angles varied from 107.2 to 122.1º which belong to acetyloxy acidic acid and indolic groups, respectively. At the same time, H-C-H and O-C-H bond angles that belong to various groups of acemetacin vary in between 107-107.3º and 105.8-111.6º, respectively. The chlorobenzoyl C-C-C-N and acetlyoxy acidic acid C-C-O-C torsional angles match with the previous values [7]. Significantly, the variations are recorded for other selected torsional angles (Table-2) compared to the previously reported values and are shown in Fig. 2.

The computed total energy, relative energy, dipole moment, the translational, rotational, vibrational, specific heat, entropy, zero-point vibrational energy (ZPVE) and rotational constants for acemetacin in gaseous and aqueous phases (water, acetone, ethanol and diethyl ether) calculated at B3LYP/6-31G(d) level of theory are given in Table-3. The polarity of a solvent can be determined by its dielectric constant. A solvent is more polar if its dielectric constant is high. Also, it is recognized that the dielectric constant plays a significant role in defining the solub-

TABLE-1
GAS AND AQUEOUS PHASE MOLECULAR GEOMETRICAL BOND LENGTHS (SELECTED) (Å) OF ACEMETACIN CALCULATED AT B3LYP/6-31G(d) LEVEL OF THEORY (FOR LABELLING OF ATOMS, FIG. 1 CAN BE REFERRED)

Bond length (Å)	Acemetacin	Acemetacin in aqueous phases			
		Water (ε = 78.5)	Acetone (ε = 20.493)	Ethanol (ε = 24.852)	Diethyl ether (ε = 4.24)
Cl1-C26	1.755	1.759	1.759	1.759	1.758
O2-C18	1.365	1.367	1.367	1.367	1.367
O2-C27	1.422	1.426	1.425	1.425	1.424
O2-C17	1.220	1.223	1.223	1.223	1.222
O2-C21	1.359	1.352	1.353	1.352	1.354
O2-C28	1.422	1.427	1.427	1.427	1.426
O2-C21	1.210	1.214	1.213	1.213	1.212
O2-C29	1.353	1.345	1.346	1.345	1.348
O2-H47	0.976	0.977	0.977	0.977	0.977
O2-C29	1.207	1.210	1.210	1.210	1.209
N8-C11	1.413	1.414	1.414	1.414	1.414
N8-C12	1.417	1.416	1.416	1.416	1.417
N8-C17	1.411	1.409	1.409	1.409	1.410
C9-C10	1.445	1.445	1.445	1.445	1.445
C9-C11	1.37	1.370	1.370	1.370	1.370
C9-C13	1.508	1.508	1.508	1.508	1.508
C10-C12	1.410	1.410	1.410	1.410	1.410
C10-C14	1.405	1.405	1.406	1.406	1.406
C11-C16	1.496	1.496	1.496	1.496	1.496
C12-C15	1.400	1.400	1.400	1.400	1.400
C13-C21	1.520	1.520	1.520	1.520	1.520
C14-C18	1.394	1.394	1.394	1.394	1.394
C15-C19	1.388	1.389	1.389	1.389	1.389
C17-C20	1.495	1.492	1.493	1.492	1.493
C18-C19	1.412	1.412	1.412	1.412	1.412
C20-C22	1.402	1.403	1.403	1.403	1.403
C20-C23	1.402	1.403	1.403	1.403	1.403
C22-C24	1.393	1.393	1.393	1.393	1.393
C23-C25	1.391	1.392	1.392	1.392	1.392
C24-C26	1.395	1.395	1.395	1.395	1.395
C25-C26	1.396	1.396	1.396	1.396	1.396
C28-C29	1.516	1.516	1.516	1.516	1.516

TABLE-2
GAS AND AQUEOUS PHASE MOLECULAR GEOMETRICAL BOND AND TORSIONAL ANGLES (SELECTED) (°) OF ACEMETACIN CALCULATED AT B3LYP/6-31G(d) LEVEL OF THEORY (FOR LABELLING OF ATOMS REFER FIG. 1)

Bond angle (°)	Acemetacin	Acemetacin in aqueous phases			
		Water (ε = 78.5)	Acetone (ε = 20.493)	Ethanol (ε = 24.852)	Diethyl ether (ε = 4.24)
Cl1-C26-C24	119.3	119.2	119.2	119.2	119.2
Cl1-C26-C25	119.3	119.2	119.2	119.2	119.2
C18-O2-C27	117.9	117.9	117.9	117.9	117.9
O2-C18-C14	124.5	124.4	124.4	124.4	124.5
O2-C18-C19	115.0	115.1	115.0	115.0	115.0
O3-C17-N8	121.0	120.8	120.9	120.9	120.9
O3-C17-C20	120.8	121.1	121.0	121.0	121.0
C21-O4-C28	115.5	116.0	116.0	116.0	115.9
O4-C21-O5	123.3	123.5	123.4	123.5	123.4
O4-C21-C13	110.8	111.1	111.1	111.1	111.0
O4-C28-C29	108.1	108.0	108.0	108.0	108.0
O5-C21-C13	125.9	125.4	125.5	125.4	125.6
O6-C29-O7	123.7	124.2	124.2	124.2	124.1
O6-C29-C28	109.4	109.4	109.4	109.4	109.4
O7-C29-C28	126.9	126.4	126.3	126.3	126.5
C11-N8-C12	108.2	108.2	108.2	108.2	108.2
C11-N8-C17	123.5	123.9	123.9	123.9	123.8
N8-C11-C9	108.8	108.8	108.8	108.8	108.8
N8-C11-C16	122.5	122.6	122.5	122.5	122.5
C12-N8-C17	127.7	127.4	127.5	127.4	127.5
N8-C12-C15	131.7	131.7	131.7	131.7	131.7

N8-C17-C20	118.1	118.0	118.0	118.0	118.1
C10-C9-C11	108.2	108.1	108.1	108.1	108.2
C10-C9-C13	125.3	125.3	125.2	125.2	125.3
C9-C10-C12	107.3	107.4	107.4	107.4	107.4
C9-C10-C14	131.9	131.8	131.9	131.9	131.9
C11-C9-C13	126.5	126.6	126.6	126.6	126.6
C9-C11-C16	128.6	128.5	128.5	128.5	128.5
C12-C10-C14	120.7	120.7	120.7	120.7	120.7
C10-C12-C15	120.7	120.8	120.8	120.8	120.8
C10-C14-C18	118.3	118.3	118.3	118.3	118.3
C17-C20-C22	122.7	122.2	122.2	122.2	122.3
C17-C20-C23	117.7	118.1	118.1	118.1	118.0
C20-C23-C25	120.7	120.6	120.7	120.7	120.7
C22-C24-C26	119.1	119.0	119.0	119.0	119.0
C20-C17-N8-C11	-148.14 [35.7[a]]	-147.92	-147.91	-147.89	-148.12
C22-C20-C17-N8	32.13 [38.0[a]]	35.49	35.27	35.30	34.55
C9-C13-C21-O4	89.68 [-172.7[a]]	88.83	89.94	89.95	89.87
C13-C21-O4-C28	-175.99 [-172.3[a]]	-176.47	-176.58	-176.59	-176.41
C21-O4-C28-C29	175.17 [-81.3[a]	174.64	178.58	178.57	178.14

[a]Taken from Ref. [11]

TABLE-3
TOTAL ENERGY E (Hartree), RELATIVE ENERGY ΔE (Kcal/mol), DIPOLE MOMENT μ_m (debye), THERMAL ENERGIES (TRANSLATIONAL (Q_T), ROTATIONAL (Q_R) AND VIBRATIONAL (Q_V) Kcal/mol), SPECIFIC HEAT (CV) (Cal/Mol-K), ENTROPY (S) (Cal/Mol-K), ZERO-POINT VIBRATIONAL ENERGY (ZPVE) (Kcal/mol) AND ROTATIONAL CONSTANTS R_A, R_B, R_C (GHz) FOR ACEMETACIN IN GASEOUS AND AQUEOUS PHASES (WATER, ACETONE, ETHANOL AND DIETHYL ETHER) CALCULATED AT B3LYP/6-31G(d) LEVEL OF THEORY

Parameters	Acemetacin	Acemetacin in aqueous phases			
		Water (ε = 78.5)	Acetone (ε = 20.493)	Ethanol (ε = 24.852)	Diethyl ether (ε = 4.24)
-E	-1777.394	-1777.411	-1777.409	-1777.410	-1777.405
ΔE	-	10.67	9.41	10.04	6.90
μ_m	3.3852	4.1645	4.0803	4.09	3.8845
Q_T	0.889	0.889	0.889	0.889	0.889
Q_R	0.889	0.889	0.889	0.889	0.889
Q_V	240.07	239.698	239.731	239.724	239.845
CV	99.256	99.488	99.466	99.471	99.388
S	186.542	187.119	186.995	187.034	186.611
ZPVE	225.05	224.633	224.669	224.661	224.801
R_A	0.2268	0.2208	0.2257	0.2257	0.2268
R_B	0.0767	0.0777	0.0768	0.0768	0.0767
R_C	0.0694	0.0706	0.0696	0.0696	0.0694

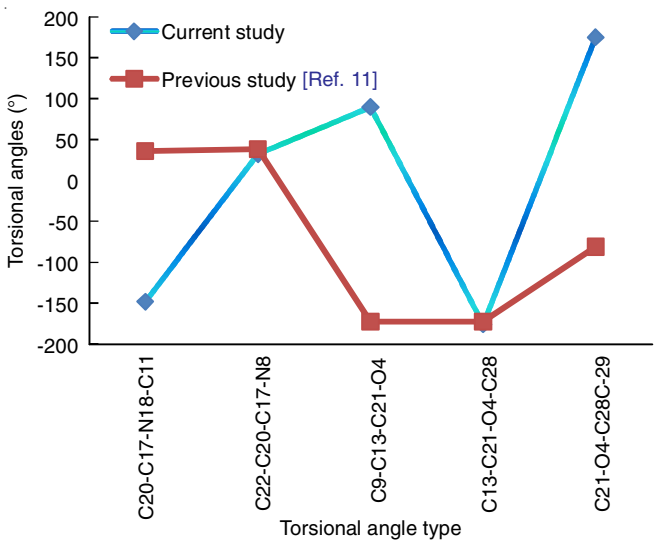

Fig. 2. Comparison of torsional angles (selected) of acemetacin with previous values

ility of molecules. The calculated energy values indicated an increase in the stability order for hydrated acemetacin (AMN) in aqueous environments as AMN-W > AMN-E > AMN-A > AMN-D, where w = water, E = ethanol, a = acetone and d = diethyl ether. It was observed that the stability of solvated acemetacin is highest in water, confirmed by its highest dielectric constant The most stable structure AMN-W is found to be more stable with respect to the least stable complex AMN-D by 3.77 Kcal/mol. The interaction of the solvents with acemetacin significantly enhanced its stability, as evidenced by a decrease in the energy values of the solvated complexes.

The ZPVE is an energy that molecules preserve even at the absolute zero temperature and it flows within molecules and governs their reactivity [15]. The ZPVE of acemetacin in gas phase is 225.05 Kcal/mol and its variation in the solvated complexes is shown in Fig. 3. The stability order predicted through the relative energies is strongly confirmed by the order based on ZPVE among the solvated acemetacin complexes, where AMN-D possesses maximum ZPVE of 224.801Kcal/mol and

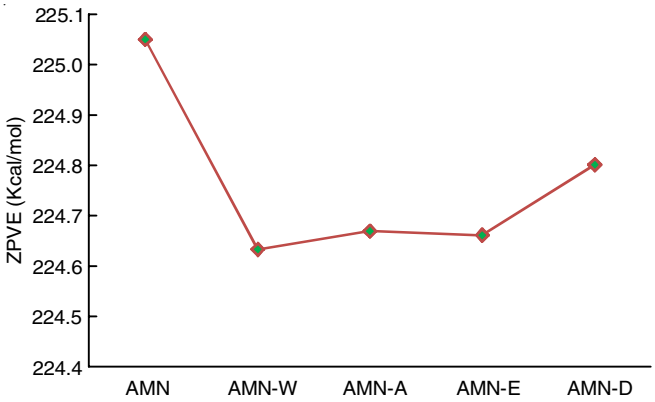

Fig. 3. Variation of zero point vibrational energy (ZPVE) of solvated acemetacin complexes

finds last place in the stability order. The computed rotational constants of acemetacin in aqueous phases demonstrated that they are mostly unaffected by the various aqueous environments. Entropy of a molecule is determined by its inherent energy, which only comes from the atoms that make up the molecule and not through interactions with atoms from other molecules as observed from the calculated entropy values of solvated acemetacin in various aqueous phases.

The ability to donate an electron is indicated by the highest occupied molecular orbitals (HOMO), which also assesses ionization potentials and is recognized as an electron donor area. The electron acceptor areas that control electron affinities and an object's ability to capture an electron are represented by the lowest unoccupied molecular orbital (LUMO). Higher HOMO values indicate that the complexes are better at donating electrons [16,17]. The ability of electron acceptance is indicated by the lower LUMO values [18]. Fig. 4 depicts the HOMO-LUMO plot for the most stable aqueous phase structure AMN-W. The HOMO is found to be localized at the chlorobenzoylic group of acemetacin where the LUMO is also positioned at chlorobenzoylic ring with a moderate contribution from the indole ring members of acemetacin.

The charge distributions of molecules are depicted in three dimensions using the electrostatic potential maps, sometimes referred to as molecular electrostatic potential (MEP) maps. The variously charged areas of a molecule can be seen from MEP. The interactions between molecules can be predicted using the charge distributions.The MEP map of the most stable solvated complex AMN-W is presented in Fig. 5. The oxygen atoms of the titled molecule fulfill the requirements to treat them as regions with affluent number of electrons, which make them favourable sites for the electrophilic interactions. The blue colour situated near the aceltyloxy acidic acid group of acemetacin makes it suitable sites for nucleophilic attacks.

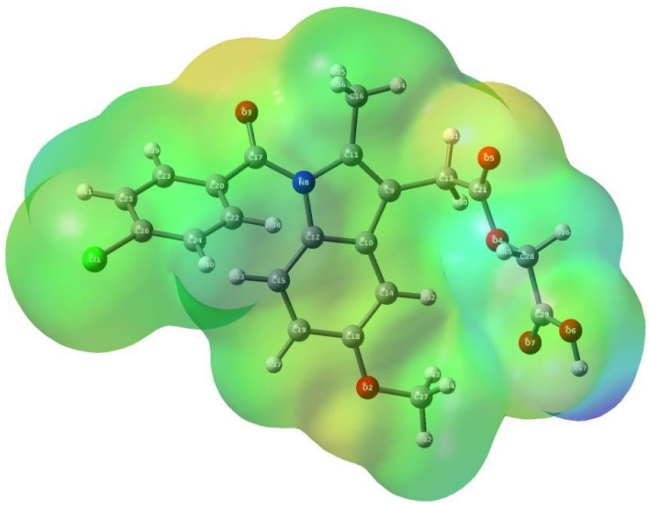

Fig. 5. Molecular electrostatic potential (MEP) mapping of AMN-W

Fig. 6 illustrates the Laplacian density distribution of the AMN-W complex, exhibiting charge concentration and charge depletion. Each contour surrounding the AMN-W molecule represents a molecular electrostatic potential (MEP) surface, with the inner contour exhibiting a higher isosurface value and the outer contour a lower one.

The B3LYP DFT method is considered to be better than other quantum chemical methods for vibrational studies [19]. Hence, the vibrational frequencies of acemetacin were analyzed and assignments have been conducted in gaseous and aqueous

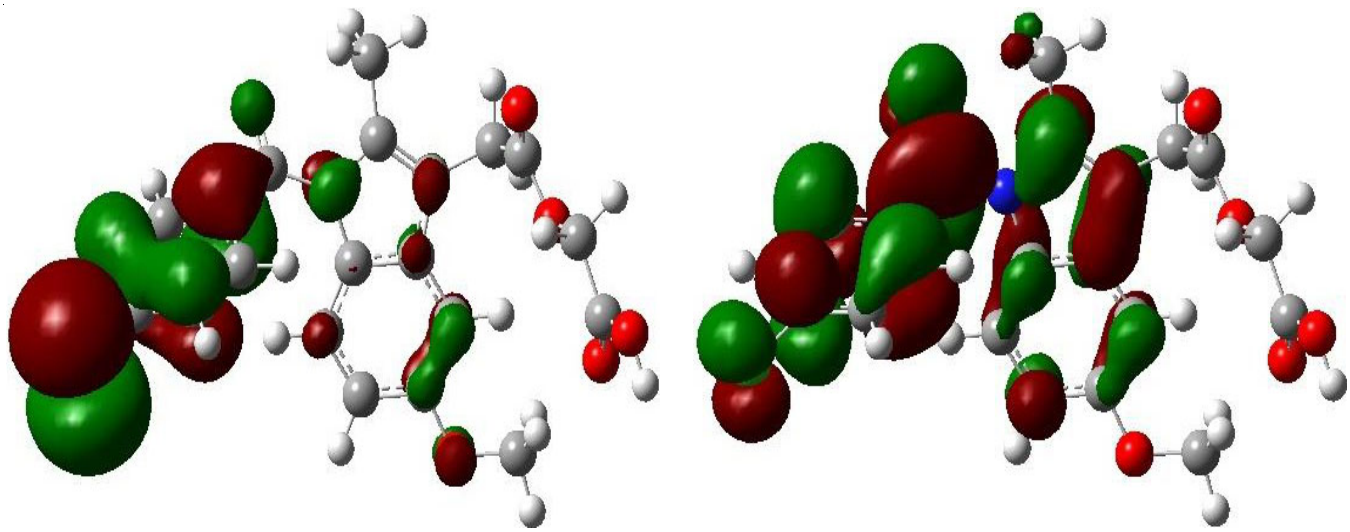

Fig. 4. Molecular orbitals for the HOMO and LUMO of AMN-W (the most stable solvated system)

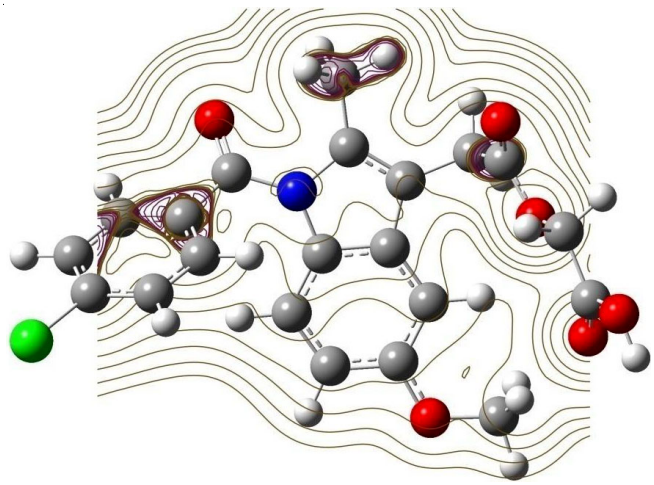

Fig. 6. The laplacian density distribution of AMN-W complex

phases through DFT-B3LYP/6-31G(d) and are shown in Table-4 (only selected values). Since acemetacin has 47 atoms and hence possesses 135 normal modes of vibrations, which are active both in infrared and Raman absorptions. The recorded IR intensities of acemetacin in gas and aqueous phases are offered in Figs. 7 and 8, respectively. The Raman intensities of the title molecule in gas and aqueous phases are shown in Figs. 9 and 10, respectively. There are no significant differences between IR intensities of acemetacin in gaseous and aqueous phases except a few. The same trend is applicable for Raman intensities also. Almost all the vibrations of acemetacin are found to be active in Raman as well as in infrared regions. The IR frequency for C=O and C-O stretch are comparable with the previously reported values [7].

The typical range for the C-H stretching is identified at 3100-3000 cm^{-1} [19]. The chlorobenzoylic, indolic, methyl,

TABLE-4
COMPUTED VIBRATIONAL FREQUENCIES (cm^{-1}) AND ASSIGNMENTS (SELECTED) FOR ACEMETACIN IN GASEOUS AND AQUEOUS PHASES BASED ON B3LYP/6-31G(d) METHOD

Gas phase	Water (ε = 78.5)	Acetone (ε = 20.493)	Ethanol (ε = 24.852)	Diethyl ether (ε = 4.24)	Vibrational Assignments
636.3	635.2	635.3	635.3	635.6	Chlorobenzoylic and indolic ring distortion
644.2	642.2	642.4	642.3	642.9	Chlorobenzoylic and indolic ring distortion
658.0	650.1	650.1	649.8	656.3	Indolic ring distortion and aceltyloxy acidic acid O-H and C-H scissoring
670.0	657.8	657.7	657.7	658.2	Aceltyloxy acidic acid O-H and C-H scissoring
681.5	679.8	680.2	680.2	680.6	Indolic ring distortion and aceltyloxy acidic acid C-H scissoring
697.2	697.9	697.7	697.7	697.7	Chlorobenzoylic ring distortion
723.3	720.6	721.0	721.0	721.8	Indolic ring distortion
748.7	746.0	746.6	746.6	747.5	Indolic and chlorobenzoylic ring distortion
750.5	748.3	749.0	748.9	749.8	Indolic and chlorobenzoylic ring distortion
765.9	764.9	764.9	764.9	765.3	Indolic and chlorobenzoylic ring distortion
805.1	805.3	805.3	805.3	805.4	Indolic C-H wagging
821.2	818.7	818.9	818.8	819.7	Chlorobenzoylic C-H wagging
843.6	842.7	843.0	843.0	843.3	Chlorobenzoylic C-H wagging
853.4	845.0	851.2	851.1	852.5	Indolic C-H twisting
860.1	852.3	856.5	856.1	861.6	Chlorobenzoylic C-H wagging
868.0	866.5	867.2	867.2	868.1	Chlorobenzoylic C-H wagging and indolic ring distorsion
888.2	890.7	890.9	890.9	890.4	Aceltyloxy acidic acid C-H rocking
925.5	923.8	923.8	923.8	924.5	Aceltyloxy acidic acid C-H rocking, indolic ring distortion and
939.3	941.3	941.1	941.1	940.8	Indolic C-H twisting
946.0	944.4	944.3	944.3	944.5	Methyl C-H rocking, chlorobenzoylic and indolic ring distortion
963.9	963.4	964.4	964.3	964.6	Chlorobenzoylic C-H twisting, methyl and aceltyloxy acidic acid C-H rocking
972.0	976.2	976.1	976.1	974.8	Chlorobenzoylic C-H twisting
978.5	979.5	979.5	979.5	979.1	Chlorobenzoylic C-H twisting
990.5	989.7	989.3	989.3	989.4	Methyl, aceltyloxy acidic acid C-H rocking and indolic ring distorsion
1032.1	1028.0	1028.3	1028.2	1029.5	Chlorobenzoylic ring distorsion, aceltyloxy acidic acid C-H rocking and indolic C-H rocking
1033.2	1032.8	1033.8	1033.8	1033.9	Chlorobenzoylic ring distorsion and aceltyloxy acidic acid C-H rocking
1038.4	1036.3	1036.2	1036.2	1036.7	Indolic, chlorobenzoylic, methyl C-H and aceltyloxy acidic acid rocking
1071.0	1061.8	1062.8	1062.7	1065.2	Methyl C-H scissoring and indolic C-H rocking
1074.6	1071.9	1071.6	1071.6	1072.0	Methyl C-H scissoring
1082.8	1075.4	1075.5	1075.5	1077.6	Methyl C-H scissoring, chlorobenzoylic ring breathing and aceltyloxy acidic acid ring distorsion
1108.0	1100.3	1100.7	1100.6	1102.6	Chlorobenzoylic ring breathing and methyl C-H rocking
1110.2	1103.3	1103.6	1103.5	1105.3	Chlorobenzoylic C-H rocking
1141.2	1140.0	1140.1	1140.1	1140.5	Chlorobenzoylic C-H scissoring
1162.4	1160.0	1160.2	1160.1	1160.7	Indolic C-H scissoring and aceltyloxy acidic acid C-H twisting
1168.5	1166.4	1166.7	1166.6	1167.1	Indolic C-H scissoring, aceltyloxy acidic acid C-H twisting and chlorobenzoylic C-H rocking
1177.6	1174.3	1174.9	1174.8	1175.5	Chlorobenzoylic C-H rocking, indolic ring distorsion and aceltyloxy acidic acid rocking

1185.6	1185.8	1184.6	1184.6	1184.5	Methoxy C-H scissoring
1194.5	1192.2	1192.1	1192.0	1192.9	Aceltyloxy acidic acid C-H twisting and indolic C-H scissoring
1211.7	1207.2	1207.6	1207.5	1208.8	Chlorobenzoylic C-H rocking
1221.0	1217.3	1217.7	1217.6	1218.7	Methoxy C-H rocking
1258.5	1256.9	1257.5	1257.5	1258.3	Aceltyloxy acidic acid C-H twisting and indolic C-H rocking
1260.8	1259.6	1260.8	1260.7	1261.1	Aceltyloxy acidic acid C-H twisting and indolic ring distorsion
1267.0	1261.7	1261.9	1262.0	1263.0	Indolic C-H rocking and ring distortion
1296.6	1290.4	1290.3	1290.3	1292.0	Aceltyloxy acidic acid C-H twisting
1297.4	1294.9	1294.6	1294.5	1295.6	Indolic ring deformation and chlorobenzoylic C-H rocking
1328.2	1327.6	1328.5	1328.4	1328.7	Indolic C-H rocking and aceltyloxy acidic acid C-H wagging
1334.0	1333.5	1333.7	1333.7	1333.9	Chlorobenzoylic C-H rocking
1335.9	1334.0	1334.7	1334.6	1335.8	Indolic C-H rocking and aceltyloxy acidic acid C-H wagging
1343.3	1339.7	1339.8	1339.7	1340.6	Indolic and chlorobenzoylic rings distorsion
1349.2	1346.1	1346.2	1346.2	1347.1	Aceltyloxy acidic acid C-H wagging and indolic ring distorsion
1352.0	1350.8	1351.7	1351.6	1351.9	Aceltyloxy acidic acid C-H wagging and indolic ring distorsion
1403.4	1401.0	1400.7	1400.6	1401.3	Indolic ring distorsion and methyl C-H scissoring
1405.4	1402.6	1402.6	1402.5	1403.3	Indolic ring distorsion
1443.1	1439.9	1440.1	1440.1	1441.0	Chlorobenzoylic C-H rocking
1445.1	1445.1	1445.1	1445.0	1446.4	Aceltyloxy acidic acid C-H scissoring
1451.9	1446.2	1446.8	1446.8	1447.1	Methyl C-H scissoring
1489.0	1485.1	1485.2	1485.1	1486.3	Indolic ring distorsion and methoxy C-H scissoring
1496.8	1490.8	1490.8	1490.6	1492.5	Aceltyloxy acidic acid and methyl C-H scissoring
1501.2	1493.2	1493.1	1493.0	1495.5	Methyl and methoxy C-H scissoring
1505.8	1497.9	1498.2	1498.1	1500.5	Acetyoxy acidic acid, methoxy and indolic C-H scissoring
1508.0	1502.1	1502.5	1502.4	1504.0	Methoxy and acetyoxy acidic acid C-H scissoring
1521.2	1513.8	1514.4	1514.3	1517.1	Methyl and acetyoxy acidic acid C-H scissoring
1523.4	1515.3	1515.1	1515.0	1517.4	Methoxy C-H scissoring
1532.6	1526.0	1526.4	1526.3	1528.3	Methoxy C-H scissoring and indole C-H rocking
1535.1	1531.7	1531.8	1531.7	1532.9	Chlorobenzoylic C-H rocking
1541.7	1533.5	1533.0	1533.0	1535.3	Methoxy C-H scissoring
1620.5	1619.2	1619.3	1619.2	1619.7	Chlorobenzoylic ring distorsion
1622.2	1619.9	1620.2	1620.1	1620.8	Indole ring distorsion
1647.5	1641.9	1642.2	1642.1	1643.8	Chlorobenzoylic ring C-C scissoring
1655.2	1651.9	1652.2	1652.2	1653.2	Indole ring distorsion
1668.0	1663.1	1663.5	1663.4	1664.7	Indole ring distorsion
1759.2	1736.9	1738.4	1738.1	1744.6	Chlorobenzoylic C=O stretching
1829.9	1799.5	1802.0	1801.6	1810.7	Acetyloxy acidic acid C=O stretching
1868.2	1838.7	1840.2	1839.8	1848.6	Acetyloxy acidic acid (COOH) C=O stretching
3031.9	3038.1	3037.9	3037.9	3036.5	Methoxy C-H (CH_3) symmetrical Stretching
3069.0	3068.5	3068.6	3068.6	3068.8	Methyl C-H (CH_3) symmetrical stretching
3076.3	3084.9	3083.9	3083.9	3081.6	Acetyloxy acidic acid C-H (CH_3) symmetrical stretching
3078.9	3086.2	3085.1	3085.3	3083.2	Acetyloxy acidic acid C-H (CH_2) symmetrical stretching
3104.1	3106.1	3105.4	3105.7	3104.9	Methoxy C-H (CH_3) asymmetrical stretching
3115.9	3124.4	3124.6	3124.6	3124.8	Acetyloxy acidic acid C-H (CH_2) asymmetrical stretching
3125.1	3129.5	3128.4	3128.6	3124.8	Methyl C-H (CH_3) asymmetrical stretching
3140.4	3144.8	3144.8	3144.9	3143.7	Acetyloxy acidic acid C-H (CH_2) asymmetrical stretching
3153.3	3155.8	3155.8	3155.9	3155.8	Methyl C-H (CH_3) asymmetrical stretching
3156.4	3162.5	3162.1	3162.2	3160.5	Methoxy C-H (CH_3) asymmetrical stretching
3215.4	3213.0	3212.9	3212.9	3213.4	Indolic C-H asymmetrical stretching
3218.6	3222.4	3222.2	3222.2	3221.3	Chlorobenzoylic C-H asymmetrical stretching
3220.3	3223.5	3223.4	3223.4	3222.7	Chlorobenzoylic C-H asymmetrical stretching
3231.9	3235.4	3235.2	3235.2	3234.2	Chlorobenzoylic C-H asymmetrical stretching
3233.2	3236.7	3236.5	3236.5	3235.6	Chlorobenzoylic C-H symmetrical stretching
3240.7	3242.9	3244.7	3244.8	3243.6	Indolic C-H asymmetrical stretching
3241.9	3245.4	3246.0	3246.0	3245.3	Indolic C-H aymmetrical stretching
3691.3	3681.7	3680.6	3680.4	3683.5	Acetyloxy acidic acid (COOH) O-H stretching

methoxy and acetlyoxy acidic acid group of acemetacin consisting of C-H bonds involve in C-H stretching vibrations. The C-H symmetrical stretching associated with its methoxy and methyl groups is observed from 3078.9 to 3031.9 cm^{-1} for the title molecule in gas phase. Significant increase in vibrational frequency values are observed for solvated acemetacin in various aqueous phases in water where 3086.2 to 3038.1 cm^{-1} are assigned to C-H symmetric stretching. For AMN-W, AMN-A and AMN-E and AMN-D complexes, these values are observed between 3245.4-3038.1 cm^{-1}, 3246-1840.2 cm^{-1}, 3246-3037.9 cm^{-1} and 3683.5-3036.5 cm^{-1}, respectively. At the same time, the asymmetrical C-H stretching of acemetacin is assigned between 3241.9 and 3104.1 cm^{-1}. This asymmetrical stretching involves various groups of acemetacin majorly involving its

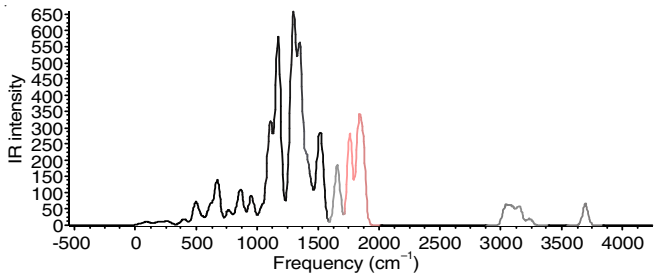

Fig. 7. Recorded IR intensities of acemetacin in gas phase

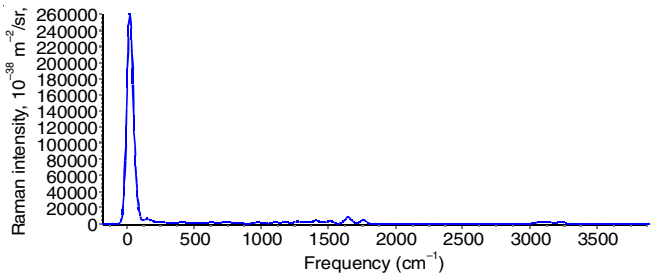

Fig. 9. Recorded Raman intensities of acemetacin in gas phase

acetyloxy acidic acid and chlorobenzoylic groups. The O-H stretching is recorded for the titled molecule at 3691.3 cm^{-1} in gas phase and interesting to observe that the aqueous medium has highly influenced the vibrational frequencies which are recorded even at the lower range.

The C-H in-plane vibrations are usually recorded in the region 1300-1000 cm^{-1} [20]. For the title compound, the C-H in-plane vibrations of methyl and methoxy groups of acemetacin such as C-H scissoring occur predominantly between 1541.7 and 1403.4 cm^{-1} in gas phase. The variations in the C-H scissoring vibrational frequencies of acemetacin in the aqueous phases are notable and presented in Table-4. One of the C-H in-plane bending vibrations of acemetacin, *i.e.* rocking calculated at B3LYP/6-31G(d) level of theory are assigned at around

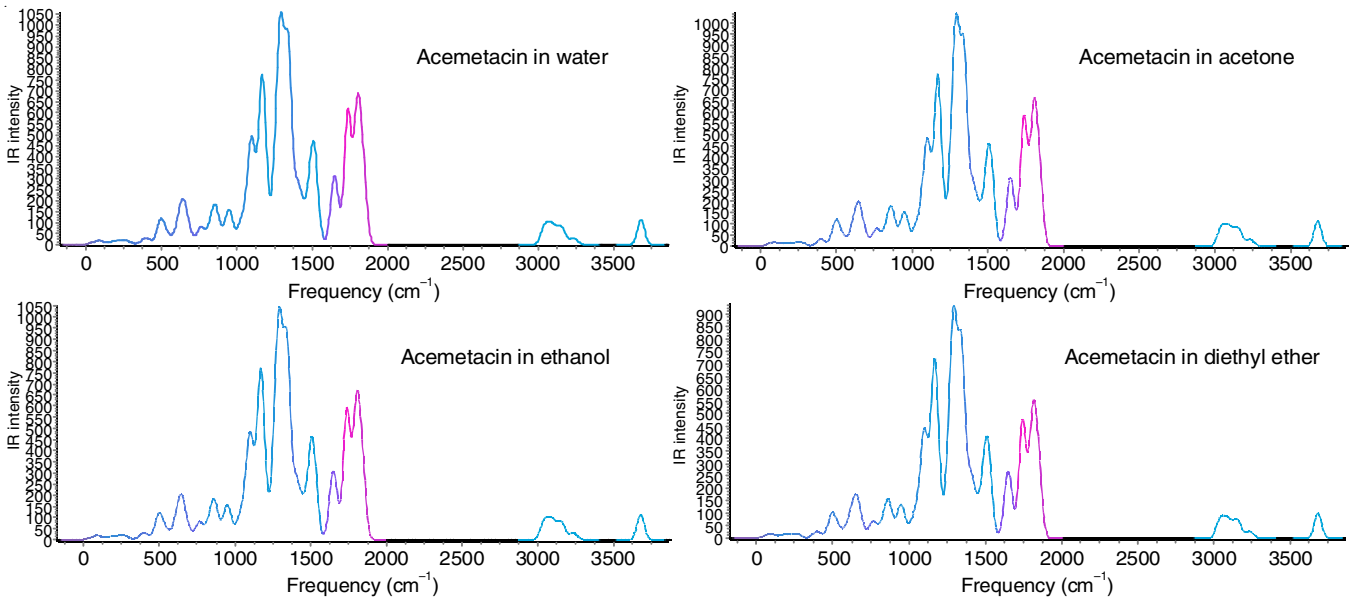

Fig. 8. Recorded IR intensities of acemetacin in aqueous phases

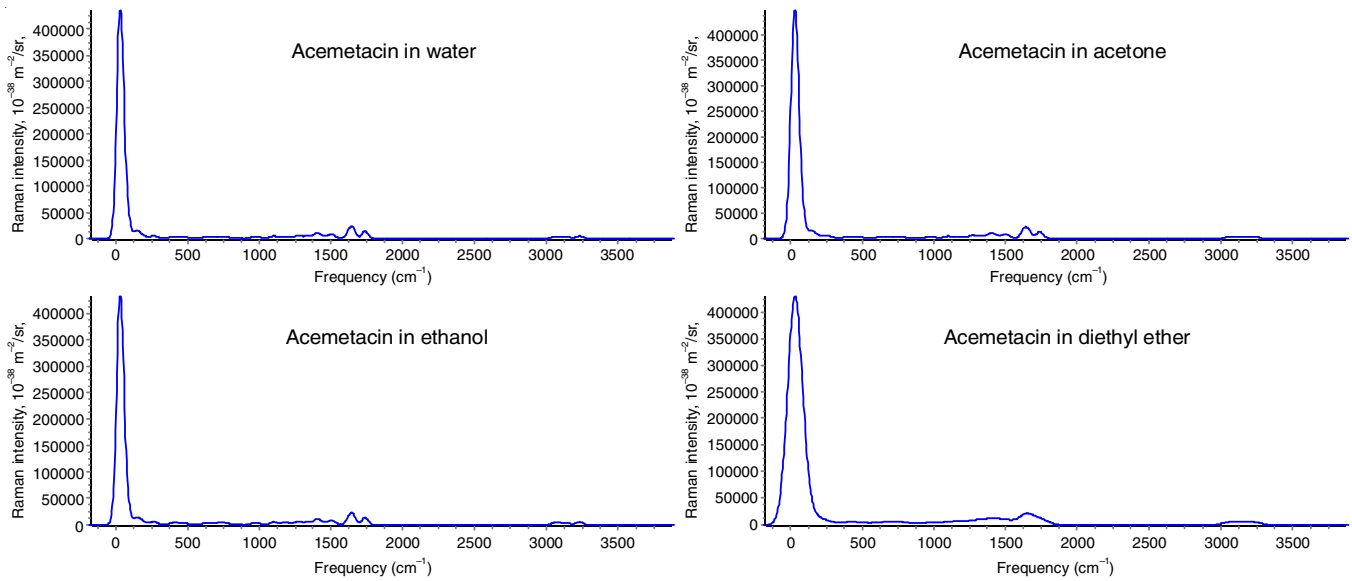

Fig. 10. Recorded Raman intensities of acemetacin in aqueous phases

1334–888.2 cm^{-1} for gas phase. The acetlyloxy acidic, methyl, indolic and chlorobenzoylic groups are characterized by C-H rocking vibrations, which are supported by a previous study that confirms this mode of vibration in the range 1100-1000 cm^{-1} [19].

The out of plane C-H vibrations (wagging and twisting) involving with indolic and chlorobenzoylic ring are verified predominantly in 805.1-868 cm^{-1} apart from 972, 978.5, 1162.4, 1168.5 and 1328.2 cm^{-1} for acemetacin in gas phase. The chlorobenzoylic, acetyloxy acidic acid and indolic rings face disturbances in terms of breathing and distortions majorly within the range of 1108–636.3 cm^{-1} and these vibrations concerning rings are significantly influenced by other vibrations.

Conclusion

In present study, the solute-solvent theoretical calculations for acemetacin in gaseous and aqueous environments were carried out in order to analyze its solubility in different non-polar solvents. The optimized geometrical parameters, thermal energies, specific heat, entropy and zero point vibrational energy of acemetacin in gaseous and aqueous phases were calculated by DFT method along with dipole moment with the purpose of getting insight into the molecular structure of acemetacin. The vibrational frequencies were computed and compared with the previously available frequencies with reasonable agreement. The HOMO-LUMO analysis helps to assess the ability of acemetacin to donate and accept electrons which influences its biological activity including its solubility. The MEP map helped to study the distribution of charge density and the chemical reactivity location of acemetacin.

CONFLICT OF INTEREST

The authors declare that there is no conflict of interests regarding the publication of this article.

REFERENCES

1. B. Berk, *J. Drug Deliv. Therap.*, **13**, 18 (2023); https://doi.org/10.22270/jddt.v13i6.5834
2. M.G. Flores, M.I. Ortiz, G.C. Hernández and A.E. Chávez-Piña, *Methods Find. Exp. Clin. Pharmacol.*, **32**, 101 (2010); https://doi.org/10.1358/mf.2010.32.2.1423883
3. R.A. Moore, S. Derry and H.J. McQuay, *Cochrane Database Syst. Rev.*, **3**, CD007589 (2009); https://doi.org/10.1002/14651858.CD007589
4. A.E. Chávez-Piña, L. Vong, W. McKnight, M. Dicay, R.C.O. Zanardo, M.I. Ortiz, G. Castañeda-Hernández and J.L. Wallace, *Br. J. Pharmacol.*, **155**, 857 (2008); https://doi.org/10.1038/bjp.2008.316
5. J.M. Chen, K.C. Liu, W.L. Yeh, J.C. Chen and S.J. Liu, *Int. J. Mol. Sci.*, **21**, 1093 (2020); https://doi.org/10.3390/ijms21031093
6. P. Sanphui, G. Bolla, U. Das, A.K. Mukherjee and A. Nangia, *CrystEngComm*, **15**, 34 (2013); https://doi.org/10.1039/C2CE26534F
7. P. Sanphui, G. Bolla, A. Nangia and V. Chernyshev, *IUCrJ*, **1**, 136 (2014); https://doi.org/10.1107/S2052252514004229
8. Y. Wang, E. Bolton, S. Dracheva, K. Karapetyan, B.A. Shoemaker, T.O. Suzek, J. Wang, J. Xiao, J. Zhang and S.H. Bryant, *Nucleic Acids Res.*, **38(suppl_1)**, D255 (2010); https://doi.org/10.1093/nar/gkp965
9. C. Lee, W. Yang and R.G. Parr, *Phys. Rev. B Condens. Matter*, **37**, 785 (1988); https://doi.org/10.1103/PhysRevB.37.785
10. J.P. Perdew and Y. Wang, *Phys. Rev. B Condens. Matter*, **45**, 13244 (1992); https://doi.org/10.1103/PhysRevB.45.13244
11. M.J. Frisch, G.W. Trucks, H.B. Schlegel, G.E. Scuseria, M.A. Robb, J.R. Cheeseman, G. Scalmani, V. Barone, B. Mennucci, G.A. Petersson, H. Nakatsuji, M. Caricato, X. Li, H.P. Hratchian, A.F. Izmaylov, J. Bloino, G. Zheng, J.L. Sonnenberg, M. Hada, M. Ehara, K. Toyota, R. Fukuda, J. Hasegawa, M. Ishida, T. Nakajima, Y. Honda, O. Kitao, H. Nakai, T. Vreven, J.A. Montgomery Jr., J.E. Peralta, F. Ogliaro, M. Bearpark, J.J. Heyd, E. Brothers, K.N. Kudin, V.N. Staroverov, T. Keith, R. Kobayashi, J. Normand, K. Raghavachari, A. Rendell, J.C. Burant, S.S. Iyengar, J. Tomasi, M. Cossi, N. Rega, J.M. Millam, M. Klene, J.E. Knox, J.B. Cross, V. Bakken, C. Adamo, J. Jaramillo, R. Gomperts, R.E. Stratmann, O. Yazyev, A.J. Austin, R. Cammi, C. Pomelli, J.W. Ochterski, R.L. Martin, K. Morokuma, V.G. Zakrzewski, G.A. Voth, P. Salvador, J.J. Dannenberg, S. Dapprich, A.D. Daniels, O. Farkas, J.B. Foresman, J. Cioslowski, J.V. Ortiz and D.J. Fox, Gaussian, Inc., Wallingford CT, Gaussian 09, revision B.01 (2010).
12. A. Frisch, A.B. Nielsen and A.J. Holder, Gauss View Molecular Visualization Program, User Manual, Gaussian Inc., Pittsburg (2001).
13. S. Miertus and J. Tomasi, *Chem. Phys.*, **65**, 239 (1982); https://doi.org/10.1016/0301-0104(82)85072-6
14. N. Rodríguez-Laguna, L.I. Reyes-García, R. Moya-Hernández, A. Rojas-Hernández and R. Gómez-Balderas, *J. Chem.*, **2016**, 9804162 (2016); https://doi.org/10.1155/2016/9804162
15. B. Abel, eds.: M.M. Martin and J.T. Hynes, The Impact of Different Molecular Environments and Chemical Substitution on Timescales of Intramolecular Vibrational Energy Redistribution in Aromatic Molecules, In: Femtochemistry and Femtobiology, Elsevier B.V., pp. 271-278 (2004).
16. M. Saranya, S. Ayyappan, R. Nithya, A. Gokila and R.K. Sangeetha, *Dig. J. Nanomater. Biostruct.*, **13**, 97 (2018).
17. M. Saranya, S. Ayyappan, R. Nithya, A. Gokila and R.K. Sangeetha, *Dig. J. Nanomater. Biostruct.*, **12**, 127 (2017).
18. B. Yogeswari, K.S. Tamilselvan, S. Thanikaikarasan, N.D. Lal, H. Anandaram, J. Madhusudhanan, R. Karthik and A. Batu, *J. Nanomater.*, **2022**, 2830708 (2022); https://doi.org/10.1155/2022/2830708
19. N. Sundaraganesan, J. Karpagam, S. Sebastian and J.P. Cornard, *Spectrochim. Acta A Mol. Biomol. Spectrosc.*, **73**, 11 (2009); https://doi.org/10.1016/j.saa.2009.01.007
20. S. Suganthi, V. Kannappan, V. Sathyanarayanamoorthi and R. Karunathan, *Indian J. Pure Appl. Phys.*, **54**, 15 (2016).